



# High-Speed Video Analysis of the Process Stability in Plasma Spraying

K. Bobzin<sup>1</sup> · M. Öte<sup>1</sup> · M. A. Knoch<sup>1</sup> · I. Alkhasli<sup>1</sup> · H. Heinemann<sup>1</sup>

Submitted: 14 June 2020 / in revised form: 31 December 2020 / Accepted: 6 January 2021 / Published online: 16 February 2021  
© The Author(s) 2021

**Abstract** In plasma spraying, instabilities and fluctuations of the plasma jet have a significant influence on the particle in-flight temperatures and velocities, thus affecting the coating properties. This work introduces a new method to analyze the stability of plasma jets using high-speed videography. An approach is presented, which digitally examines the images to determine the size of the plasma jet core. By correlating this jet size with the acquisition time, a time-dependent signal of the plasma jet size is generated. In order to evaluate the stability of the plasma jet, this signal is analyzed by calculating its coefficient of variation  $c_v$ . The method is validated by measuring the known difference in stability between a single-cathode and a cascaded multi-cathode plasma generator. For this purpose, a design of experiment, covering a variety of parameters, is conducted. To identify the cause of the plasma jet fluctuations, the frequency spectra are obtained and subsequently interpreted by means of the fast Fourier transformation. To quantify the significance of the fluctuations on the particle in-flight properties, a new single numerical parameter is introduced. This parameter is based on the fraction of the time-dependent signal of the plasma jet in the relevant frequency range.

**Keywords** diagnostics · high-speed video analysis · multi-cathode · plasma spraying · process stability · single cathode

## Abbreviations

SC	Single cathode
MC	Multi-cathode
FFT	Fast Fourier transformation
th	Threshold
$\dot{V}$	Plasma gas flow rate
$I$	Electrical current
$\mu$	Mean plasma jet size
$\sigma$	Standard deviation
$c_v$	Coefficient of variation
$\delta_{\text{fluct}}$	Fraction of fluctuations below 10,000 Hz

## 1 Introduction

Thermal spraying cumulates processes that use an energy source to heat and accelerate a gas, its thermal and kinetic energy melts and accelerates a spray material with the purpose of forming a coating on a surface (Ref 1). These coatings can increase the functional performance of a surface, such as heat resistance, corrosion and oxidation resistance and electrical properties, as well as improve the lifespan of components by a higher wear resistance (Ref 2). Thermal spraying also offers the opportunity to apply a coating of specialized alloys for certain applications onto low cost materials. Plasma spraying is part of the coating processes in the group of thermal spraying. The plasma jets used in plasma spraying exhibit high temperatures of up to 20,000 K, allowing to apply coatings of almost any congruently melting solid material onto various substrate

**Supplementary Information** The online version contains supplementary material available at <https://doi.org/10.1007/s11666-021-01159-1>.

✉ H. Heinemann  
heinemann@iot.rwth-aachen.de

<sup>1</sup> Surface Engineering Institute, RWTH Aachen University, Kackertstr. 15, 52072 Aachen, Germany

materials (Ref 3). According to Fauchais et al., these reasons lead to the conclusion that plasma spraying is one of the most versatile coating technologies (Ref 4), with the only limitation that the melting temperature of the processed material needs to be at least 300 K below its temperature for vaporization or decomposition, in order to avoid low deposition efficiencies (Ref 5).

The energy used for the generation of the thermal plasma in plasma spraying originates from an electric arc (Ref 6). The generators utilized to create the thermal plasmas are highly dynamic systems, an exemplary setup can be seen in Fig. 1. Interactions between the flow drag and electromagnetic forces affect the root position of the plasma column. In combination with turbulence, this leads to a constantly moving plasma column within the plasma chamber, causing an instable power output, and therefore result in time-dependent plasma jet properties as shown by Coudert et al. (Ref 7).

The purpose of the plasma jet is to heat and accelerate the injected particles. If the temperatures and the size of the jet fluctuate over time, it inevitably alters the temperatures, velocities and trajectories of the sprayed particles, as studied by Park et al. (Ref 8) in numerical simulations and further investigated in experimental measurements by Bisson et al. (Ref 9). In Fig. 2 (Video in the supplementary files), the mentioned influence of the plasma jet fluctuations on the particle injection is visualized. The upper part of the images shows the injector outlet, from which the particles flow in the direction of the plasma jet. In the lower part of the images, part of the plasma jet can be seen, which is

flowing from the left to the right. In the first image, the particles penetrate into the plasma jet perpendicularly. Over the course of the next images, the particle stream is bent by an upcoming wave of the plasma jet. This change of the particle trajectory results in varying properties of the in-flight particles. Consequently, the instabilities of the plasma jet contribute to the inhomogeneity of plasma sprayed coatings and are, therefore, of major interest for the further process development as discussed by Bisson and Moreau (Ref 10).

The fluctuations of the arc attachment point are certainly the main cause for the instabilities of the plasma jet. Numerous publications investigating the stability of the plasma spraying process correlated the movement of the electric arc with the temporally varying potential differences (Ref 11–14). However, in some novel torch designs (i.e., TriplexPro™ or DELTA), the plasma is created by more than one electric arc and the superposing effects of multiple electric arcs render it difficult to identify the influence of these separate arcs on the plasma jet. In addition, the jet stability outside of both plasma torches is affected by turbulences and air entrainment as demonstrated by Pfender et al. (Ref 15). Furthermore, according to relatively new discussion published by Heimann (Ref 16), the highly nonlinear nature of the plasma process and up to 60 intrinsic and extrinsic process parameters prevent a reproducibility of the coating properties by only controlling the process parameters. In order to observe the behavior of the plasma jet and thus the plasma spraying

**Fig. 1** Influence of the plasma jet fluctuations on the particle injection. MC plasma generator,  $I = 200$  A,  $\dot{V} = 50$  SLPM Ar

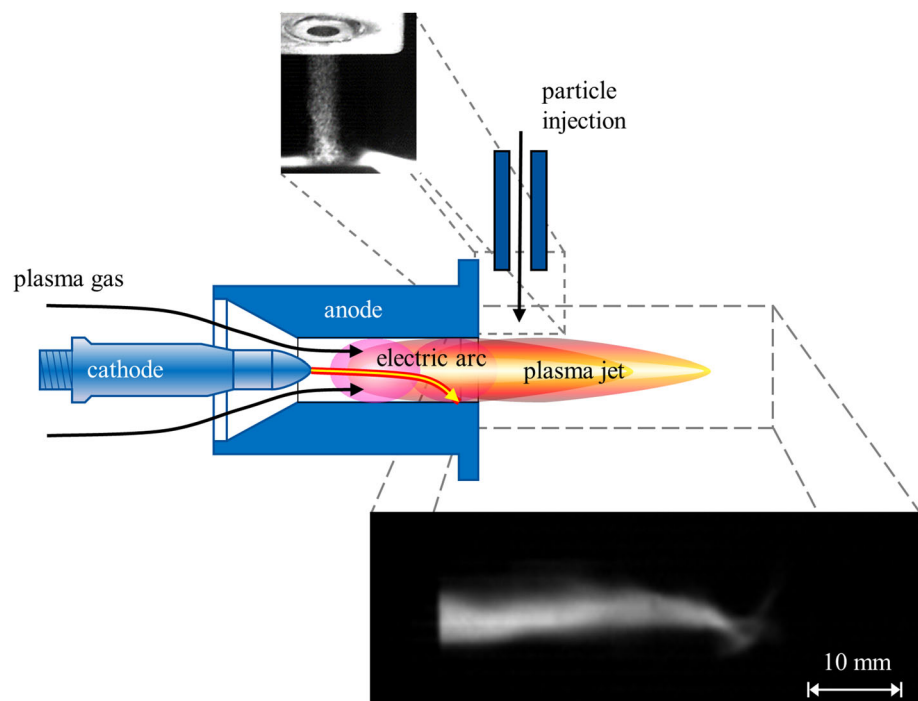
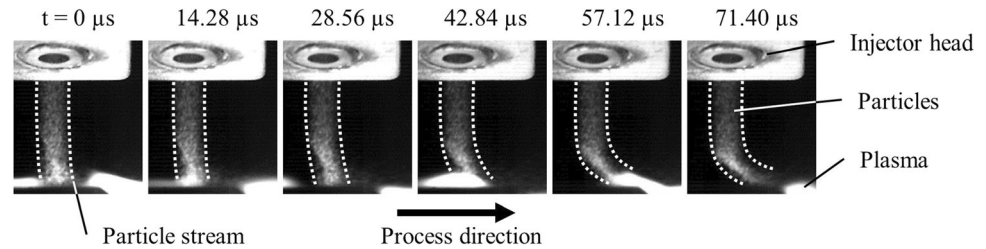


**Fig. 2** Experimental setup of the plasma torch and the high-speed (HS) camera with an exemplary image of the single-cathode plasma jet (video is attached in the supplementary files)



process comprehensively, Samukawa et al. demanded the development of new methods for its diagnostic (Ref 17).

To target the aforementioned matters, this work presents a new approach for the examination of plasma jet fluctuations based on high-speed videography. An investigation of the plasma spraying process by means of a video analysis is not a novel concept and has already been proposed in the early nineties by Fauchais et al. (Ref 18) and Agapakis and Hoffman (Ref 19). To observe the movement of the plasma column, some authors recorded head-on images of single-cathode plasma generators. Likewise, Dorier et al. (Ref 20) studied the azimuthal position of the arc attachment point at the anode of a single-cathode plasma torch. With these recordings, they were able to show the complex nature of the anodic arc attachment point movement. In the same way, Duan and Heberlein (Ref 21) used high-speed head-on images to determine the arc attachment position and the thickness of the cold-gas layer between the plasma column and the nozzle wall to correlate these results with the different arc operating modes.

Similarly, observations of the plasma spraying process with the help of optical analyses have been conducted previously. Brogan et al. (Ref 22) used pulsed lasers to observe the particle flow into the plasma jet and Raghu et al. (Ref 23) combined this with the Schlieren imaging method to additionally capture the plasma jet. The same Schlieren imaging technique was used by Fincke et al. (Ref 24) to investigate the flow field and the air entrainment. Russ et al. (Ref 25) qualitatively compared the images of a plasma jet with the arc voltage signal. They observed that stronger fluctuations of the arc voltage lead to increased instabilities of the plasma jet. Comparable work was conducted by Tiwari et al. (Ref 26), who observed a delay between the voltage signal and the apparent jet size. Hlína et al. (Ref 27) analyzed the spatial distributions of oscillations in a plasma jet by applying the FFT on the images of a CCD camera and later improved the method using the wavelet analysis (Ref 28). However, these investigations of the jet stability were limited to recording frequencies of up to 8000 Hz due to the available hardware. Dorier et al. (Ref 14) related high-frequency measurements of the optical emissions of the plasma jet with the arc voltage. They found a strong correlation between the voltage and the emission signal. While giving

new insights into plasma jet stability, these investigations did not evaluate the stability of the plasma jet in its entirety. Nowadays, state-of-the-art equipment is capable of capturing images of the plasma jets at significantly higher recording frequencies as demonstrated by Ondac et al. (Ref 29). Thus, the aim of this study is to develop a new method that enables a quantitative evaluation of the plasma jet stability, based on state-of-the-art high-speed videography.

For this purpose, the raw images are digitally processed to measure the apparent plasma jet size. In a first step, this method is qualified using two common torches with different electrode configurations, i.e., a single-cathode (SC) and a cascaded multi-cathode (MC) plasma spraying torch. Schein et al. (Ref 30) described that MC plasma torches result in a significantly more stable plasma jet. One reason for the increased stability of the former plasma jet is the cascaded design of the anode in the MC generator: By inserting a neutral electrode (neutrode) between the cathode and the anode, the arc is extended and fixed, as shown by Marqués et al. (Ref 31). This leads to a higher arc voltage and lower voltage fluctuations, in turn resulting in a more stable power dissipation to the plasma jet. The second reason for the increased plasma jet stability of the MC generator is the generation of the plasma by three separate arcs instead of one. By dividing the electrical power into three arcs, the fluctuations of the three arcs are super positioned and the power dissipation into the plasma is spatially distributed. This, together with the cascaded anode design, allows a generation of the more stable plasma jet—an improved coating homogeneity is the expected outcome. Since this difference between the SC and MC generator is known, the measurements in this paper were applied to these two plasma torches in order to qualify the developed method. Furthermore, a design of experiment is conducted to estimate the influence of different operating parameters. Using FFT, the frequency spectra are obtained and the apparent fluctuation frequencies are identified. Combining this information with the calculated mean particle residence time, a single parameter, which enables the evaluation of the influence of jet stability on the sprayed particles, is derived.

In the following, the developed method and its functionality are described in detail. Subsequently, the

experimental setup, the used equipment and the process parameters are presented. At the end of this paper, the results are discussed and conclusions are drawn.

## 2 Qualitative and Quantitative Plasma Jet Analysis

A high-speed camera is employed to take videos of the plasma jet at a distance of 0.5 m from the torch axis. The resulting images represent the core of the plasma jet, where the high temperatures lead to a visible emission of light. Two different methods to analyze these high-speed videos are described here: a qualitative and a quantitative one. The former is only described here for the sake of completeness and for interested readers. It was not used further in this article, as it is more suitable for giving an impression to an audience. The latter was used to evaluate the high-speed recordings presented in the section results.

The first presented approach to evaluate the plasma jet stability is rather qualitatively. The method is based upon the idea to record a video of the plasma jet at different frequencies, visually examine these videos and decide if the jets appear stable at that given recording frequency. However, by lowering the frequency the exposure time is raised. This leads quite fast to plain white images because of the bright plasma emissions. It is possible to compensate this effect by lowering the exposure time independently of the frequency or with neutral-density filters. However, in the first case only short sequences of the events are recorded, which leads to a significant loss of information especially for huge differences between the frequency and the exposure time. In case of the neutral-density filters, the videos have to be taken at different times, and thus unique disturbances, which correspond to separate events in the jet stream, will appear only in some of the recordings. These unique events can compromise an analysis, as they prevent a direct comparability between the different recordings taken at varying frequencies.

These drawbacks can be circumvented by recording the images at the highest possible frequency and then digitally editing the original video to obtain the same effect. The high temporal resolution allows to capture even events which are very short in time, thus prevents a smearing of such events. At the same time, the digital merging allows an evaluation of one unique experimental result at different timescales. The processing is based on the original recorded picture set with the highest frequency. To create a video with half the frequency, for every time step of the new video, two subsequent pictures of the original sequence are merged as shown in Fig. 3.

The merger is done by setting the value of each pixel in the new video to the mean value of the original two pixels

at this position. This allows the digital creation of a new video with half of the original frequency. The procedure can be further iterated until only one picture is left. These digitally edited videos can be analyzed qualitatively giving a subjective assessment of the jet stability. Possible insights are, however, limited to the frequencies obtained during the digital editing. Nevertheless, this method enables a quick and easy evaluation of the jet fluctuations, by overwhelming the over-exposure problem at low recording frequencies. Likewise, this method gives a good optical impression of the plasma jet stability, which can be presented to an audience. Therefore, this method was described in this paper for readers, who are potentially interested in evaluating plasma jet behavior under different temporal resolutions.

This paper focuses on the quantitative approach, which digitally processes the images to measure the apparent size of the plasma jet core. The videos of the plasma jet are again recorded with the highest possible frequency of the capturing device to provide the highest temporal resolution. In the next step, the recorded pictures are converted into black and white images. The conversion is displayed in Fig. 4. (Please find also the video attached in the supplementary files.) It is realized using the `imbinarize()` function of the MATLAB software package using a threshold (`th`) as input parameter. All pixel with a value above this threshold are converted into a white pixel, the rest become black ones, with  $th = 1$  being the maximum possible bit value of the pixel and  $th = 0$  being the lowest possible value. In case of the later used image depth of 12 bit a threshold of  $th = 1$  would mean that only pixels with a value of  $2^{12} = 4096$  are converted to white pixels. The fundamental idea of this conversion is to only capture the temporal development of an arbitrary hot core region of the plasma jet. These hotter regions of the plasma jet are capable of melting the particles and are therefore its fluctuations are of interest. Another approach would be to evaluate the intensity of all pixels and thus create one total intensity pixel value. However, thereby areas at the fringe of the plasma jet with no significant influence on the particles would be included into the analysis. In addition, it must be considered that the optically visible areas correspond to a projection of three-dimensional plasma jet. Since the optical path through the center of the plasma jet is longer than in the peripheral areas, the center would appear brighter even if it has the same temperature. Based on these reasons, the analysis in this work was carried out using the presented conversion.

The processed images are then evaluated by counting the number of white pixels, giving a numerical value that represents the plasma jet size for each frame. These values represent in this context the visible area of the plasma jet and thus does not reflect the volume of the plasma jet. This

**Fig. 3** Schematic overview of the image merger

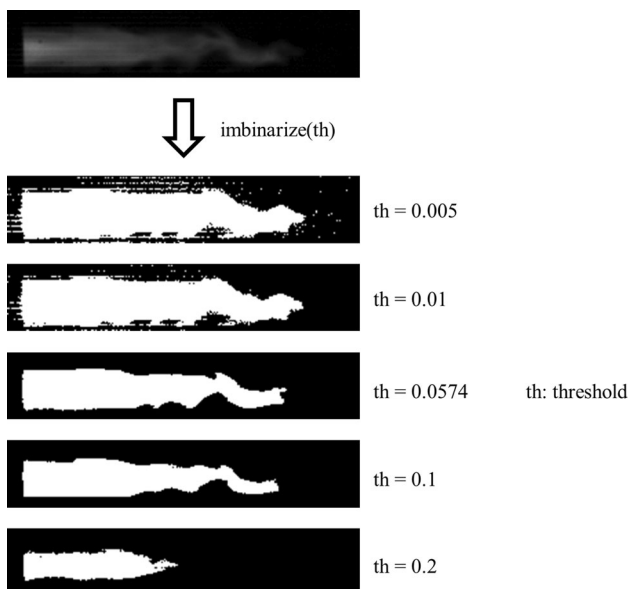
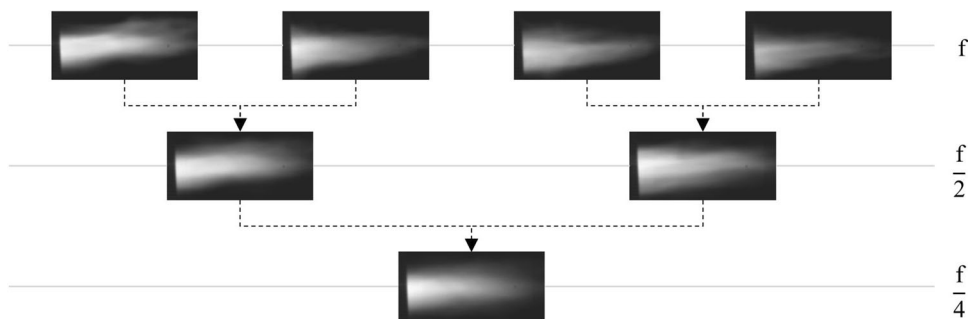


**Fig. 4** Conversion of a 12-bit picture into a 1-bit black and white picture with the `im2bw()` function for different thresholds. MC plasma generator,  $I = 425$  A,  $\dot{V} = 110$  SLPM Ar (video is attached in the supplementary files)

value is correlated with the acquisition time, generating a time-dependent signal for the plasma jet size. Thereby, a numerical investigation of the plasma jet stability becomes feasible. An example of this signal, with the corresponding black and white images, is given in Fig. 5.

While this signal clearly shows the presence of fluctuations, their frequencies are not evident in this representation. Therefore, the transformation of this signal into the frequency domain, with the help of the FFT, is used to reveal the predominant frequencies. The FFT decomposes the signal into its frequency components. As a result, the prevailing frequencies and their magnitudes are obtained and represented in a frequency spectrum. In case of the considered plasma jet, the FFT analysis enables the determination of the frequency and the significance of the plasma jet size fluctuations, thus helping to identify the origin of these instabilities. By combining this information with the mean time of flight of a given particle, the relevance of these fluctuations, regarding coating

homogeneity, can be estimated as well. This approach will be further described in the following.

### 3 Experimental Setup

The quantitative method was applied to investigate two different plasma torch variants, i.e., a MC and SC plasma generator. For each plasma torch, five different parameter sets are analyzed to determine, whether the parameter choice has an influence on the stability of the plasma jet. These parameters are listed in Table 1, representing a  $2^2$  factorial design with one center point.

The two incorporated process parameters are the plasma gas flow rate ( $\dot{V}$ ) and the electric current ( $I$ ). An argon and hydrogen gas mixture was used for the SC plasma generator. Hydrogen is necessary in most thermal spraying applications for SC torches, as it increases the heat transfer to the particles (Ref 6). In case of the MC plasma generator, only argon was employed as plasma gas. This is feasible, as the MC plasma generator has a higher power output and can, therefore, process high-melting materials without adding hydrogen. The employed SC plasma torch is the F4-XMBL, Oerlikon Metco, with an anode/nozzle diameter of 6 mm. The TriplexPro™-210, Oerlikon Metco, with an anode/nozzle diameter of 9 mm is utilized for the investigation of a MC plasma torch. The different nozzle diameters and plasma gas mixtures can surely lead to different flow conditions at the nozzle outlet, thus affecting the jet stability. Nevertheless, these nozzle diameters were chosen as they represent the conventionally used diameters for the respective torch type and are therefore commonly used in coating processes of ceramics.

The videos were recorded with the camera Photron Fastcam SA5 1000K as 12-bit greyscale pictures with a frame rate of 325,500 Hz and an exposure time of 1  $\mu$ s using a Nikon ED AF Micro NIKKOR 200mm 1:4 D lens. The recorded images have a size of  $265 \times 56$  pixel with an optical resolution of about 0.3 mm/pixel, thereby representing an optical field of 76.8 mm  $\times$  16.8 mm. The recorded videos have a length of 100,000 frames or

**Fig. 5** Size of the plasma jet represented by the number of white pixel over the time and corresponding black and white images. SC plasma generator,  $I = 500$  A,  $\dot{V} = 70$  SLPM Ar + 10 SLPM H<sub>2</sub> with a threshold of 3.125%

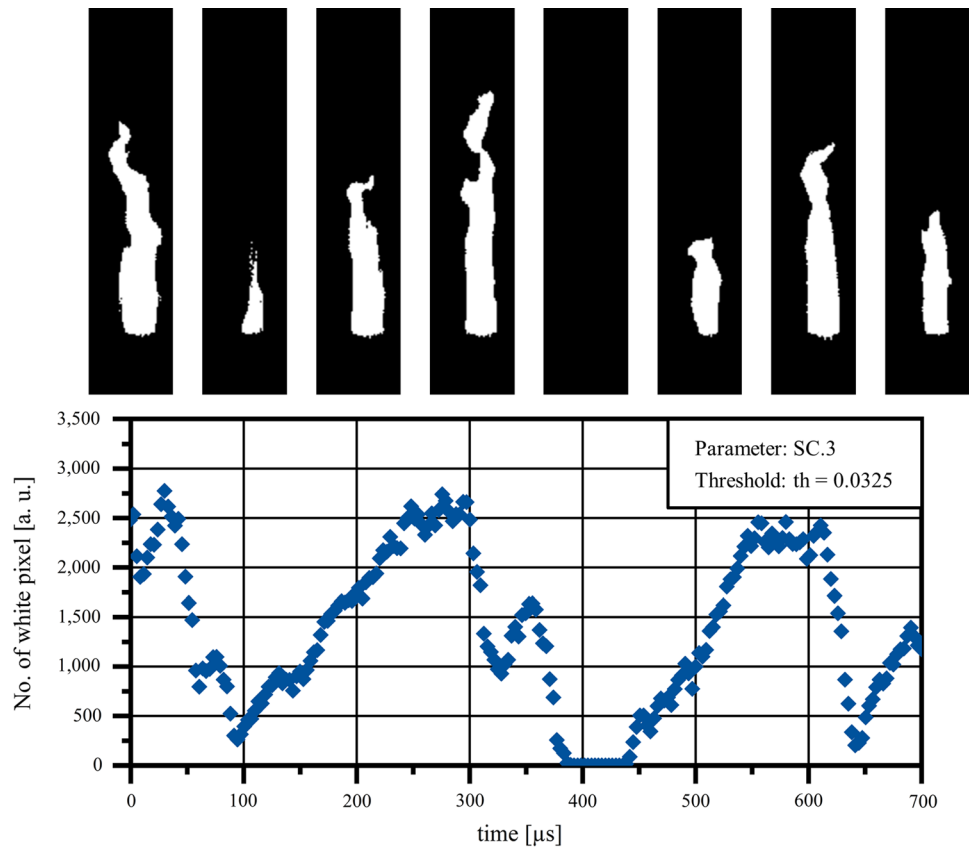


**Table 1** Process parameters and corresponding voltage and net power levels

Torch type	Parameter	$I$ , A	Level	$\dot{V}$ Ar/H, slpm	Level	$U$ , V	$P_{net}$ , kW
Single-cathode plasma torch (SC)	SC.1	400	–	40/8	–	62.5	14.9
	SC.2	400	–	100/12	+	83.8	22.7
	SC.3	500	0	70/10	0	73.6	23.9
	SC.4	600	+	40/8	–	62.9	24.6
	SC.5	600	+	100/12	+	81.4	32.7
Multi-cathode plasma torch (MC)	MC.1	350	–	70	–	91.0	20.8
	MC.2	350	–	150	+	114.1	28.9
	MC.3	425	0	110	0	109.3	34.4
	MC.4	500	+	70	–	102.5	31.3
	MC.5	500	+	150	+	125.4	42.4

0.3072 s. To compensate the unequal bright plasma jets of the MC and SC torches, different neutral density filters were mounted on the lens. For the SC plasma torch, an ND8 filter was used, which transmits 12.5% of the incident light. In case of the MC plasma torch, a stack of ND8 and ND4 was necessary. The combination of these two filters led to a fractional transmittance of 3.125%. The choice of the threshold has a substantial effect on the resulting images. If chosen too high, only small parts of the core of the plasma jet are considered in the following analysis, whereas a too low choice results in images greatly

disturbed by noise and an overestimation of the jet size. The thresholds therefore were determined using the Otsu's method (Ref 32), a standard method to binarize images, on the first 1000 images of the process parameters MC.2 and SC.2 and calculating an average threshold value. For the digital processing, a threshold of  $th_{MC} = 0.0574$  was determined for the images taken with the MC plasma torch and a threshold of  $th_{SC} = 0.2038$  in case of the SC plasma torch for the MATLAB function `imbinarize()`. The chosen method appears to result in an appropriate trade-off between noise and jet size (see Fig. 4).

### 4 Results and Discussion

After converting the images, the resulting signals were statistically analyzed. The results are listed in Table 2. The mean size values ( $\mu$ ) represent the mean value of the core size of the plasma jet over time. Due to the different ND-filters, these mean values are not comparable between the different plasma torches. Furthermore, different plasma gas mixtures were used in the factorial experiment for the SC generator and the emission coefficient of the argon/hydrogen plasma heavily depends on the Ar/H<sub>2</sub> ratio. Increasing H<sub>2</sub> contents increases the emission coefficients of the plasma gas and thus the apparent plasma jet size should increase as well. However, the Ar/H<sub>2</sub> ratio does not change significantly, and thus, its influence on the visual plasma jet appearance is neglected. Consequently, the influence of different process parameters on the mean size values ( $\mu$ ) of the plasma jet can be evaluated. The size of the plasma jet is expectedly bigger for higher magnitudes of electric currents and hence for higher power levels. On the contrary, the measured mean size of the plasma jet becomes smaller for high gas flow rates. These results were rather expected, as the higher power level results in a larger volume of plasma emitting visible light and higher gas flow rates lead to lower plasma temperatures, thus reducing the apparent plasma jet size.

Although mean values can give some insights about the influence of process parameters on the size of the plasma jet, for the evaluation of the plasma jet stability, the mean values are rather irrelevant. The stability can be evaluated by considering the deviations of the jet size signals from the calculated mean value. Consequently, the standard deviation ( $\sigma$ ) could give a measure for the plasma jet stability. However, it provides a value of the total fluctuations and as the jet sizes vary for the different torches and process parameters,  $\sigma$  cannot be used for a comparison of these. Therefore, it is necessary to normalize the signal of the mean size value or to normalize the deviations, by

using the coefficient of variation ( $c_v$ ), which is defined as the ratio between the standard deviation and the mean of the jet size signal:  $c_v = \frac{\sigma}{\mu}$ . This compensates the effects of different emissions or attenuation filters and enables a comparison of the signals for different torch designs as well as for different parameter sets. Yet we must keep in mind that for absolute comparability, all settings need to be as equal as possible.

In Fig. 6, the signals of the jet sizes for the SC and MC plasma generators are shown exemplary for parameter set 4 over a time sequence of 5 ms. The jet sizes were normalized to achieve a graphic comparability, by dividing the signal by its mean value and then shifting it to the y-axis, using the following equation:

$$\text{signal}_{\text{normalized}}(t) = \frac{\text{signal}(t)}{\mu_{\text{signal}}} - 1.$$

The difference between the two plasma torches is clearly evident. While the normalized jet size signal of the SC plasma generator varies strongly between  $\pm 0.75$ , with peaks of up to  $\pm 1$ , the signal of the MC plasma stays within a range of  $\pm 0.25$ . As the fluctuations of the SC plasma jet exceed the fluctuations of the MC plasma jet by far, this gives a first indication that the used method to quantify the stability with the help of high-speed videography leads to the valid results. The expected difference between the more stable plasma jet of the MC and that of the SC generator can be detected.

This difference can be quantified using the  $c_v$ . In Fig. 7, these coefficients are displayed for both plasma torches and parameter sets. Again, the difference between the MC and SC plasma generator, shown in two colors, is evident. For the SC plasma generator, the  $c_v$  shows values between 0.560 and 0.772, whereas the  $c_v$  of the MC plasma generator ranges between 0.067 and 0.176. Thereby, it can be stated that with the introduced methodology the plasma jet instabilities can be described with a single numerical value, which can be

**Table 2** Statistic values of the jet size signals

Parameter	Mean size $\mu$ , pixel	SD $\sigma$ , pixel	Coefficient of variation $c_v$ , a.u.
SC.1	765	590.1	0.772
SC.2	687	478.8	0.697
SC.3	869	625.8	0.720
SC.4	1438	805.4	0.560
SC.5	1084	684.4	0.632
SC <sub>mean</sub>	969	636.9	0.676
MC.1	3460	279.0	0.080
MC.2	2568	452.1	0.176
MC.3	3938	288.9	0.073
MC.4	4974	334.0	0.067
MC.5	4384	321.3	0.073
MC <sub>mean</sub>	3865	335.1	0.094

**Fig. 6** Comparison of the evolution of the plasma jet size for the single- and multi-cathode plasma generator for the parameter set 4

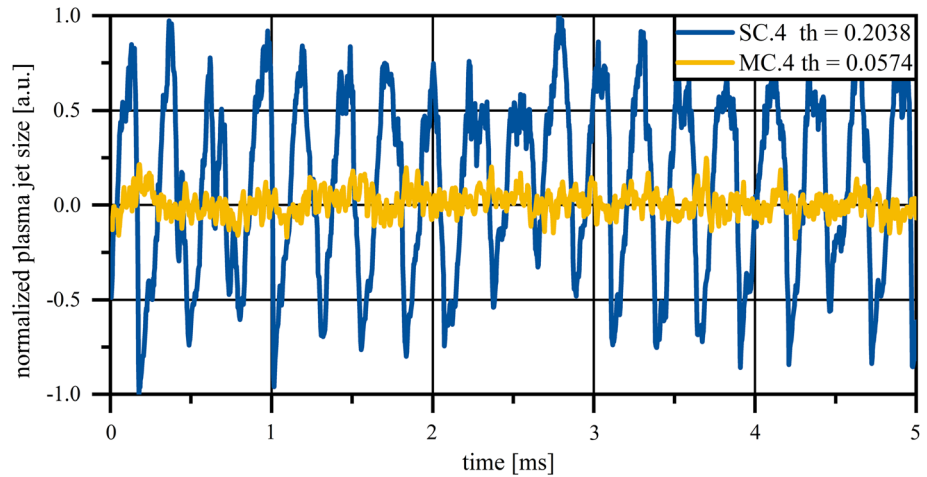
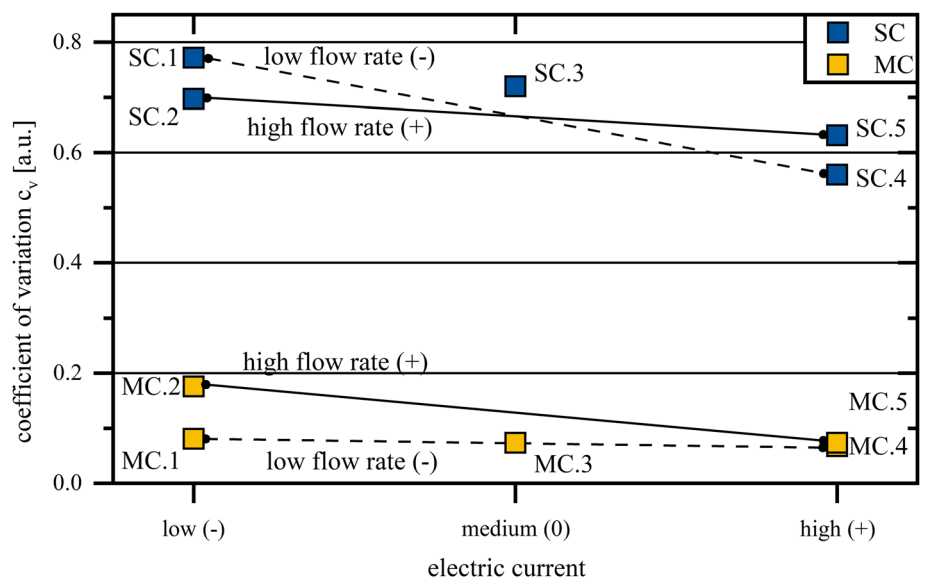


**Fig. 7** Coefficient of variation ( $c_v$ ) of the plasma jet size for different parameter sets. The threshold for the conversion was 3.125%



used to quantitatively compare the jet stability of different plasma spraying systems. However, the comparison between the plasma troches must still be treated with caution, as the recordings were taken using different ND filters and consequently different thresholds were used. The parameters SC.2 and MC.1 may be the most comparable. In this case, as well, the difference between the two generator types is distinct.

The horizontal axis of Fig. 7 shows the influence of the electric current ( $I$ ) on the  $c_v$  values. The lines connect process parameters with the equal plasma gas flow rates ( $\dot{V}$ ): The solid line denotes the high flow rates (+) and the dashed line the lower flow rates (–) as shown in Table 1. The two single points with the parameter sets 3 (SC/MC.3) represent the center points with medium current (0) and medium flow rate (0). It can be seen in Fig. 7 that plasma jets generated by process parameters with higher magnitudes of electric current are more stable, than the ones generated with lower magnitudes of electric currents.

The more stable behavior can be explained by considering the mean size values  $\mu$  of the plasma jets in Table 2. While the standard deviation  $\sigma$  is more or less comparable for all process parameters, the size of the plasma jet varies significantly and exhibits higher mean values for the parameters with higher electric currents. Thus, as the plasma jet is larger in size due to the increased current, the occurring fluctuations have less influence on the stability of the plasma jet. Similar can be observed in case of the flow rate ( $\dot{V}$ ). Lower flow rates lead to larger plasma jet sizes. Therefore, the apparent fluctuations have a smaller influence on the jet, leading to lower values of  $c_v$ . The opposite is valid for higher flow rates. However, this cannot be observed for parameter SC.2 and SC.1. In this case, the parameter with the lower flow rate exhibits a higher value of  $c_v$ . A possible explanation is that the increased argon flow leads to a reduction of the arc attachment zone at the anode and thus a more stable arc in case of parameter SC.2.



The reason for this is the increasing drag forces exerted by the cold gas in the boundary layer.

The jet size signals were analyzed using the FFT, allowing further investigation of the jet instabilities as the signal is transformed into the frequency domain. The frequency spectrum can help to identify the cause of the fluctuations, as well as their influence on the jet stability. In Fig. 8, the frequency spectra of the SC and MC plasma generator are exemplary displayed for the parameter set 4. Note that the spectra are normalized to their respective highest peak. For all parameter sets of the SC plasma generator, a distinct oscillation frequency in the range between 3000 and 3800 Hz and its first harmonic can be observed; the exact values of the peak frequencies are given in Table 3.

These peaks are located in the typical frequency range for an electric arc operating in the restrike mode in a SC plasma generator, first described by Eckert et al. (Ref 33) in 1967 and later substantiated through investigations conducted by Duan and Heberlein (Ref 21) and Rat et al. (Ref 34) for a variety of SC plasma generators. The periodic movement of the electric arc of an argon and hydrogen plasma lead to a highly oscillating arc voltage. The resulting instable power dissipation affects the plasma jet and is therefore evident in the values of  $c_v$  and in the frequency spectrum. The apparent frequency peak is highly dominant in the frequency spectrum. Thus, the restrike

mode seems to be the main reason for the observed plasma jet instabilities in case of the SC torch.

Additionally, a smaller peak at 300 Hz is observable in the frequency spectra. This peak is caused by the rectification of the alternating current to the direct current, which is used for the plasma torches. The power line frequency is 50 Hz, after rectification of the three phases in the power supply, a 300 Hz ripple remains, which is in accordance to reported ripples in the literature (Ref 35). This ripple is then present in the plasma fluctuations as well. In case of the MC plasma generator, this 300 Hz peak is the only apparent peak. However, the 300 Hz peak is rather small and narrow for both plasma torch designs; therefore, its influence on the jet stability can be neglected. The detection of this peak is yet of significance, since this observation is proof of the sensitivity of the applied method.

For the MC plasma generator, no dominant frequency oscillations are apparent, apart from the 300 Hz ripple. The more randomly distributed fluctuations of the plasma jet can be attributed to the design of the MC plasma torch. Generally, the distance between cathode and anode is higher for this torch type, causing a higher arc voltage. Similarly, the anode is shorter, restricting the arc movement and consequently the arc voltage fluctuations to a lower level. Furthermore, the torch operates with three electric arcs and the effects of these three arcs superpose. As a result, the plasma is heated more uniformly and is

**Fig. 8** Frequency spectra of the SC and MC plasma generator for the parameter set 4 up to 20,000 Hz. The spectra were normalized to their highest peak

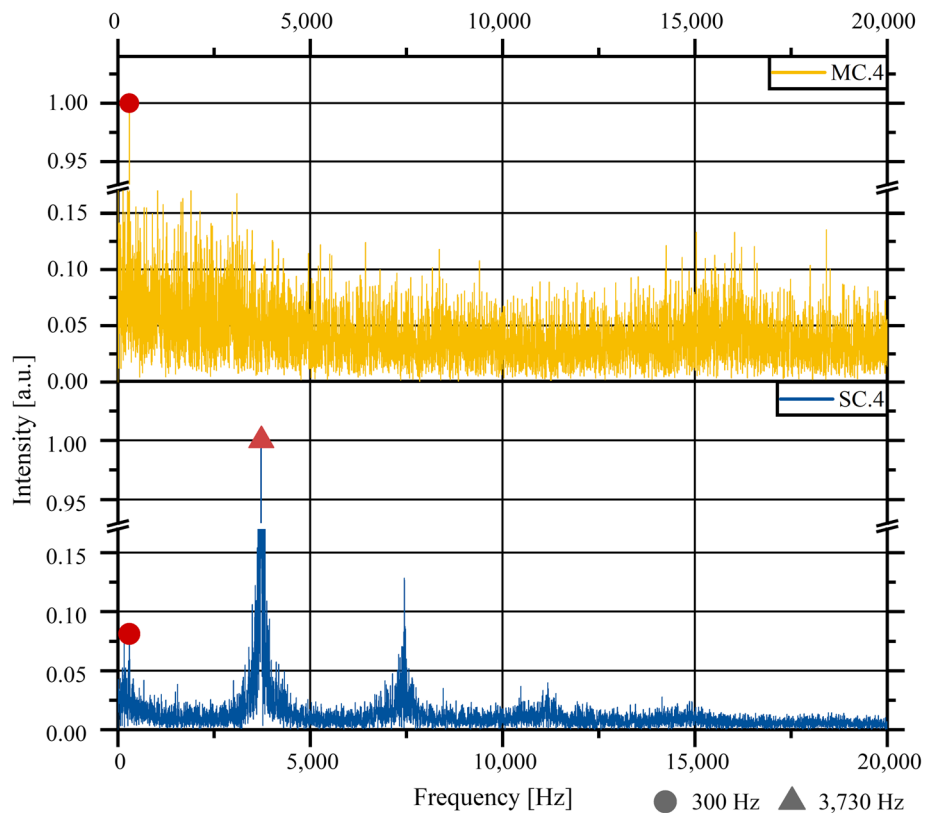


**Table 3** Values for the peak frequency of the jet size signal ( $f_{\text{peak}}$ ), the ratio of fluctuations over 10,000 Hz ( $\delta_{\text{fluct}}$ ) and the multiplication of the coefficient of variation ( $c_v$ ) with  $\delta_{\text{fluct}}$ ,  $c_{v,\text{fluct}}$

Parameter	$f_{\text{Peak}}$ , Hz	$\delta_{\text{fluct}}$ , a.u.	$c_{v,\text{fluct}}$ , a.u.
SC.1	3076	0.423	0.326
SC.2	3086	0.337	0.235
SC.3	3291	0.388	0.280
SC.4	3730	0.457	0.256
SC.5	3388	0.416	0.263
SC <sub>mean</sub>	...	0.404	0.272
MC.1	300	0.270	0.022
MC.2	300	0.309	0.054
MC.3	300	0.240	0.018
MC.4	300	0.250	0.017
MC.5	300	0.229	0.017
MC <sub>mean</sub>	...	0.260	0.025

therefore more stable. However, it is not clear whether the three distinct arcs or the greater distance between the cathode and the shorter anode contribute more to this stabilizing effect. As the present fluctuations are irregular, it seems reasonable that they are mainly caused by turbulence effects.

The purpose of the plasma jet is to heat and accelerate the particles. Therefore, only the fluctuations significantly influencing the particle properties are of interest. To determine this influence, it is necessary to know the residence time of the injected particles in the plasma jet. Hence, simulations of the plasma-particle interaction with an existing model of the authors (Ref 36, 37) were used to get the first estimation about the particle residence time in a plasma jet. The simulations were conducted for a MC plasma torch, but the calculated residence times are expected to be in the same range for a SC torch for comparable parameters. The results indicate a mean residence time in the plasma jet of roughly 1 ms for alumina with a mean particle diameter of  $d_{\text{mean}} = 38 \mu\text{m}$ . This is in accordance with the particle residence times reported in literature: in general a few milliseconds by Fincke and Swank (Ref 38), in particular in the range of 0.25–1.25 ms for zirconia by Fauchais et al. (Ref 39), and 0.4–1.4 ms for alumina by Vardelle et al. (Ref 40). In Fig. 9, the possible influence of the plasma jet fluctuations on the particles is illustrated. The three blue lines represent the jet size for pure sinusoidal oscillations with frequencies of 500, 1000 and 10,000 Hz. The bars at the top of the figure represent the residence times of the particles, which are injected at an arbitrary time.

With the help of this figure, it can be imagined that, in case of a plasma jet fluctuating at a frequency of 500 Hz, the first particle would be subjected to higher temperatures

as it is injected when the plasma jet exhibits a maximum in size. On the other hand, the next particle, which is injected 1 ms later, will be moving into the plasma jet when the size and power level of the plasma jet is smaller. Therefore, it is evident that fluctuations of 500 Hz would have a great impact on the particles' properties. Jet size fluctuations with a frequency of 1000 Hz would reduce this influence and would lead to a more homogenous treatment of the particles injected at arbitrary times as illustrated in the figure. Obviously, this is only a conceptual illustration which neglects the relative motion between the particles and the plasma jet. Yet, it can be stated that the influence of the fluctuations on the particles decreases with increasing oscillation frequencies, as the particles undergo multiple maxima and minima. A possible threshold for influence of oscillations on the particles should also cover shorter residence times of faster particles due to different diameters or operating parameters. Therefore, in this work it is assumed that plasma jet fluctuations of one order of magnitude faster than the calculated particle residence time would have only an insignificant influence on the heating and accelerating of different particles. This corresponds to a frequency of 10,000 Hz. While it is a rather arbitrary value, it represents a conservative boundary for this investigation.

To determine the proportion of fluctuations below 10,000 Hz of the total fluctuations, the frequency spectra (Fig. 8) are evaluated in more detail. The spectrum is divided into two parts by integrating up to 10,000 Hz ( $C_{10k}$ ) and comparing this value to the integral from 0 to 162,750 Hz ( $C_{\text{total}}$ ). The ratio  $\frac{C_{10k}}{C_{\text{total}}}$  represents the fraction of oscillations below 10,000 Hz compared to the entire spectrum in a single numerical value  $\delta_{\text{fluct}} = \frac{C_{10k}}{C_{\text{total}}}$ . High  $\delta_{\text{fluct}}$  values indicate that the instabilities of the plasma jet appear mostly in a frequency range affecting the particle properties upon impact on the substrate. Thus, small values are more favorable. The calculated  $\delta_{\text{fluct}}$  values are shown in Fig. 10. It is evident that  $\delta_{\text{fluct}}$  values are higher in the case of the SC plasma torch; they vary between  $\delta_{\text{fluct}} = 0.337$  and  $\delta_{\text{fluct}} = 0.457$ . On the contrary, the  $\delta_{\text{fluct}}$  values of the MC plasma torch are in the range of  $\delta_{\text{fluct}} = 0.229$  to  $\delta_{\text{fluct}} = 0.309$ . The mean  $\delta_{\text{fluct}}$  value of the SC plasma torch is  $\delta_{\text{SC}} = 0.404$  and  $\delta_{\text{MC}} = 0.260$  for the MC plasma generator. The reason for the high values of the SC generator is the fluctuations of the restrike mode, which operates within the considered frequency range of up to 10,000 Hz. Likewise, the more randomly distributed frequency spectrum of the MC plasma torch results in lower  $\delta_{\text{fluct}}$  values.

In order to measure the influence of plasma jet fluctuations on the particles, the two above-mentioned values  $c_v$  and  $\delta_{\text{fluct}}$  can be combined to a single indicator by multiplication. This new indicator  $c_{v,\text{fluct}} = c_v \cdot \delta_{\text{fluct}}$  represents

**Fig. 9** Illustration of the influence of jet size fluctuations with different frequencies on a particle with a residence time in the plasma jet of 1 ms for different times of injection

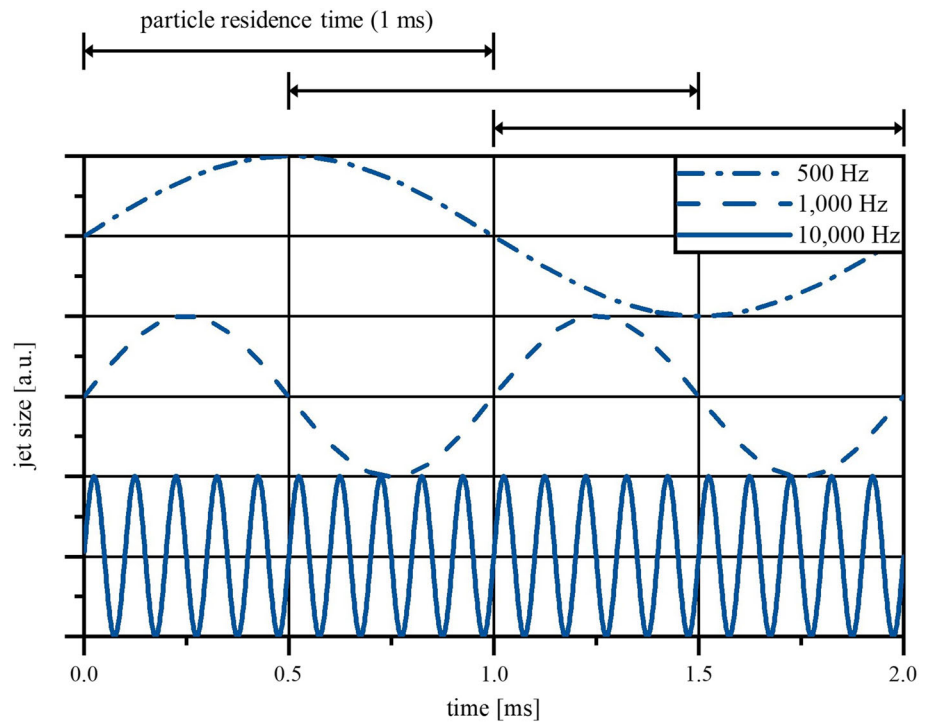
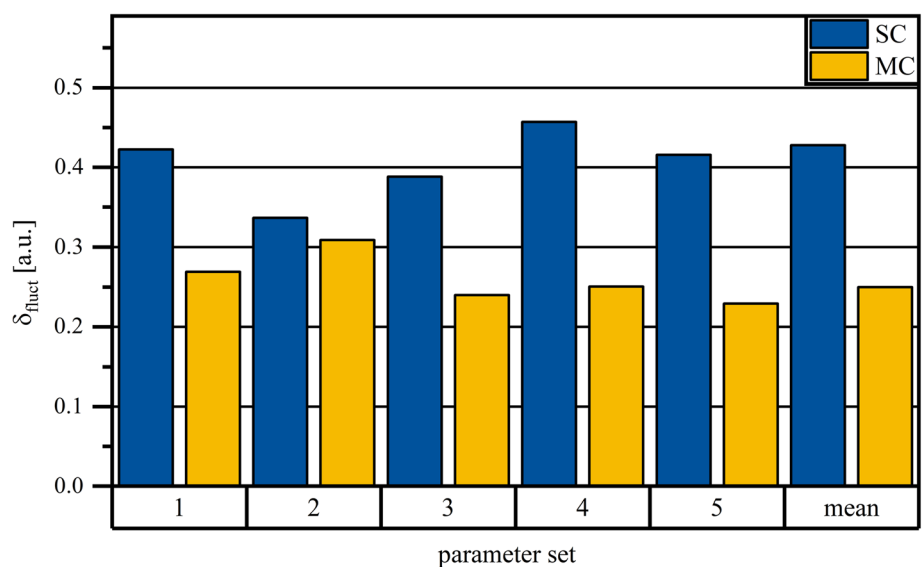


**Fig. 10** Fraction of the frequency spectrum below 10,000 Hz  $\delta_{fluct}$ , for the different torches and parameter sets

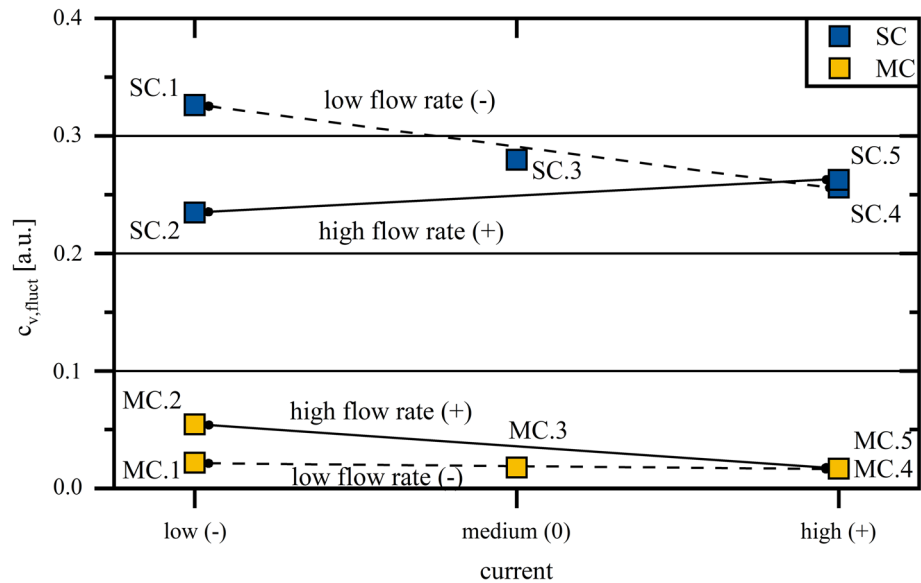


the coefficient of variation which is corrected by the amount of fluctuations in the frequency range affecting the injected particles of below 10,000 Hz. In contrast  $c_v$  was a measure for all occurring fluctuations independent of its frequency. This new indicator  $c_{v,fluct}$  is shown in Fig. 11 for the different parameter sets. Again, apart from the parameter SC.1 and SC.2, the effects of the process parameters, electrical current ( $I$ ) and flow rate ( $\dot{V}$ ) on  $c_{v,fluct}$  show the same tendencies as for the values of the  $c_v$ . Likewise, the difference between the two torch designs is clearly visible and even larger then in case of  $c_v$ . The already lower

fluctuations of the MC torch seem to have a lower effect on the particles. However, this result needs to be verified in the future using particle diagnostics.

The presented results substantiate the known fact that the MC plasma torch is more stable than the SC torch. Not only the  $c_v$ , which represents the relative magnitude of the fluctuations of the jet are smaller, these fluctuations are also predominantly found in a higher frequency domain, which reduces their influence on the sprayed particles. The  $c_{v,fluct}$  values indicate that the influence of the jet size fluctuations on the in-flight particle properties could be up

**Fig. 11** Values of  $c_{v,\text{fluct}} = c_v \delta_{\text{fluct}}$  for different plasma torches and process parameters



to 80% lower for the MC plasma generator compared to the industrial standard, the SC generator. Yet these results need to be validated using a different methodology.

## 5 Conclusion

A high-speed camera was used to observe the plasma jet fluctuations and thus the process stability of two different DC plasma generators. Two methods were presented to evaluate these fluctuations: a qualitative and a quantitative approach. The latter method was applied, as it digitally processes the recorded images, allowing for a statistical analysis of the plasma jet behavior in a quantifiable manner. In a first step, the method was validated by detecting the known difference in stability between the two plasma torch designs. Furthermore, the method was capable of quantifying this difference using the coefficient of variation,  $c_v$ , which gives a measure of the stability of plasma jets. Additionally, it was shown that the dominant oscillation frequencies can be determined by FFT. In case of the SC plasma generator, the typical restrike peak between 3000 and 4000 Hz was observed. For both torch designs, the 300 Hz rectification ripple was tracked, proving the sensitivity of the employed method. In a further step, the frequency spectra were re-evaluated to estimate the influence of the determined instabilities on the particle properties. A new statistical value  $\delta_{\text{fluct}}$  was defined to quantify the proportion of fluctuation in the relevant frequency range. In this work, the relevant frequency range was chosen rather conservatively to be up to 10,000 Hz. By multiplying the two values  $c_v$  and  $\delta_{\text{fluct}}$ , the plasma jet instabilities affecting the injected particles can be quantified with a single numerical value  $c_{v,\text{fluct}}$ . This value

indicated a significantly lower effect of the higher frequent fluctuations of the MC plasma generator on the in-flight particles. To sum up the results, the increased plasma stability of a MC plasma generator was quantified using only optical method. This result is in accordance with many years of experience, giving credence to the presented method.

In a next step, a third torch type, a cascaded single-cathode plasma generator, should be evaluated. This could reveal whether in case of the MC torch the three arcs or the cascaded design of the anode contribute more to the increased plasma jet stability. Furthermore, the different parameters regarding electrical current, gas flow rate and gas mixture should be evaluated in more detail to confirm the observed tendencies. In particular, argon hydrogen mixtures shall be used with the MC torch and argon only mixtures on the SC torch. These investigations should then be combined with measurements of the arc potential, arc current and the particle properties temperature and velocity. In addition to these planned studies, the methodology can be further improved: The frequency range for  $\delta_{\text{fluct}}$  could be narrowed down to a range that is still relevant for the particle properties, thus increasing the precision of the method. Likewise, the shape of the plasma free jet could be taken into account for the evaluation of the high-speed images.

In conclusion, the use of a high-speed camera can improve the analysis of plasma torches. Not only the effects of the electric arc on the plasma jet are captured, additionally the influence of turbulence, air entrainments and other extrinsic or intrinsic process parameters can be observed. New torch designs or nozzle outlets, addressing these topics to improve the jet stability, could be assessed with this method or with further modifications of this

method. Another possible application is the online control of the plasma spraying process: the stability and reproducibility could be monitored, leading to an improved coating homogeneity and quality.

**Acknowledgments** The presented investigations were carried out at RWTH Aachen University within the framework of the Collaborative Research Centre SFB1120-236616214 “Bauteilpräzision durch Beherrschung von Schmelze und Erstarrung in Produktionsprozessen” and funded by the Deutsche Forschungsgemeinschaft e.V. (DFG, German Research Foundation). The sponsorship and support is gratefully acknowledged. The authors would like to thank the Fraunhofer Institute for Laser Technology (ILT), Aachen for providing the camera equipment.

**Funding** Open Access funding enabled and organized by Projekt DEAL.

**Open Access** This article is licensed under a Creative Commons Attribution 4.0 International License, which permits use, sharing, adaptation, distribution and reproduction in any medium or format, as long as you give appropriate credit to the original author(s) and the source, provide a link to the Creative Commons licence, and indicate if changes were made. The images or other third party material in this article are included in the article’s Creative Commons licence, unless indicated otherwise in a credit line to the material. If material is not included in the article’s Creative Commons licence and your intended use is not permitted by statutory regulation or exceeds the permitted use, you will need to obtain permission directly from the copyright holder. To view a copy of this licence, visit <http://creativecommons.org/licenses/by/4.0/>.

## References

1. L. Pawłowski, *The Science and Engineering of Thermal Spray Coatings*, 2nd ed. Wiley, New York, 2008
2. R.C. Tucker Ed., *Thermal Spray Technology*, 2nd ed. ASM International, Novelty, 2013
3. J.R. Davis Ed., *Handbook of Thermal Spray Technology*, 1st ed. ASM International, Novelty, 2004
4. P.L. Fauchais, J.V. Heberlein, and M.I. Boulos, *Thermal Spray Fundamentals: from Powder to Part*, Springer, Berlin, 2014
5. P.L. Fauchais, Understanding Plasma Spraying, *J. Phys. D Appl. Phys.*, 2004, **37**(9), p R86-R108
6. R.B. Heimann, *Plasma Spray Coating: Principles and Applications*, 2nd ed. Wiley, New York, 2008
7. J.-F. Coudert, M.P. Planch, and P.L. Fauchais, Velocity Measurement of DC Plasma Jets Based on Arc Root Fluctuations, *Plasma Chem. Plasma Process.*, 1995, **15**(1), p 47-70
8. J.H. Park, J.V. Heberlein, E. Pfender, Y.-C. Lau, J. Ruud, and H.P. Wang, Particle Behavior in a Fluctuating Plasma Jet, *Ann. N. Y. Acad. Sci.*, 1999, **891**(1), p 417-424
9. J.F. Bisson, B. Gauthier, and C. Moreau, Effect of Plasma Fluctuations on In-Flight Particle Parameters, *J. Therm. Spray Technol.*, 2003, **12**(1), p 38-43
10. J.F. Bisson and C. Moreau, Effect of Direct-Current Plasma Fluctuations on In-Flight Particle Parameters: Part II, *J. Therm. Spray Technol.*, 2003, **12**(2), p 258-264
11. J.-F. Coudert, V. Rat, and D. Rigot, Influence of Helmholtz Oscillations on Arc Voltage Fluctuations in a DC Plasma Spraying Torch, *J. Phys. D Appl. Phys.*, 2007, **40**(23), p 7357-7366
12. L. Leblanc and C. Moreau, The Long-Term Stability of Plasma Spraying, *J. Therm. Spray Technol.*, 2002, **11**(3), p 380-386
13. S. Janisson, A. Vardelle, J.-F. Coudert, P.L. Fauchais, and E. Meillot, Analysis of the Stability of DC Plasma Gun Operating With Ar-He-H<sub>2</sub> Gas Mixtures, *Ann. N. Y. Acad. Sci.*, 1999, **891**(1), p 407-416
14. J.-L. Dorier, C. Hollenstein, A. Salito, M. Loch, and G. Barbezat, Characterisation and Origin of Arc Fluctuations in a F4 DC Plasma Torch Used for Thermal Spraying, *High Temp. Mater. Process.*, 2001, **5**(4), p 13
15. E. Pfender, J.R. Fincke, and R. Spores, Entrainment of Cold Gas into Thermal Plasma Jets, *Plasma Chem. Plasma Process.*, 1991, **11**(4), p 529-543
16. R.B. Heimann, A Discussion on the Limits to Coating Reproducibility Based on Heat Transfer Instabilities, *J. Therm. Spray Technol.*, 2019, **28**(3), p 327-332
17. S. Samukawa, M. Hori, S. Rauf, K. Tachibana, P. Bruggeman, G. Kroesen, J.C. Whitehead, A.B. Murphy, A.F. Gutsol, S. Starikovskaia, U. Kortshagen, J.-P. Boeuf, T.J. Sommerer, M.J. Kushner, U. Czarnetzki, and N. Mason, The 2012 Plasma Roadmap, *J. Phys. D Appl. Phys.*, 2012, **45**(25), p 253001
18. P.L. Fauchais, J.-F. Coudert, M. Vardelle, A. Vardelle, and A. Denoirjean, Diagnostics of Thermal Spraying Plasma Jets, *J. Therm. Spray Technol.*, 1992, **1**(2), p 117-128
19. J. Agapakis and T. Hoffman, Real-Time Imaging for Thermal Spray Process Development and Control, *J. Therm. Spray Technol.*, 1992, **1**(1), p 19-25
20. J.-L. Dorier, M. Gindrat, C. Hollenstein, A. Salito, M. Loch, and G. Barbezat, Time-Resolved Imaging of Anodic Arc Root Behavior During Fluctuations of a DC Plasma Spraying Torch, *IEEE Trans. Plasma Sci.*, 2001, **29**(3), p 494-501
21. Z. Duan and J.V. Heberlein, Arc Instabilities in a Plasma Spray Torch, *J. Therm. Spray Technol.*, 2002, **11**(1), p 44-51
22. J.A. Brogan, C.C. Berndt, W.C. Smith, R.V. Gansert, S. Raghu, S. Sampath, and H. Herman, Real-Time Imaging of the Plasma Spray Process—Work in Progress, *J. Therm. Spray Technol.*, 1995, **4**(4), p 374-376
23. S. Raghu, G. Goutevenier, and R. Gansert, Comparative Study of the Structure of Gas-Stabilized and Water-Stabilized Plasma Jets, *J. Therm. Spray Technol.*, 1995, **4**(2), p 175-178
24. J.R. Fincke, D.M. Crawford, S.C. Snyder, W.D. Swank, D.C. Haggard, and R.L. Williamson, Entrainment in High-Velocity, High-Temperature Plasma Jets Part I: Experimental Results, *Int. J. Heat Mass Transf.*, 2003, **46**(22), p 4201-4213
25. S. Russ, P.J. Strykowski, and E. Pfender, Mixing in Plasma and Low Density Jets, *Exp. Fluids*, 1994, **16**(5), p 297-307
26. N. Tiwari, S.N. Sahasrabudhe, N.K. Joshi, and A.K. Das, Study of Jet Fluctuations in DC Plasma Torch Using High Speed Camera, *J. Phys. Conf. Ser.*, 2010, **208**, p 12134
27. J. Hlína, J. Sonsky, and V. Nenicka, Mapping of Spatial Distributions of Oscillations in a Thermals Plasma Jet, *High Temp. Mater. Process.*, 2004, **8**(2), p 215-220
28. J. Hlína, J. Gruber, and J. Šonský, Application of a CCD Camera to Investigations of Oscillations in a Thermal Plasma Jet, *Meas. Sci. Technol.*, 2006, **17**(4), p 918-922
29. P. Ondac, A. Maslani, and M. Hrabovsky, Investigation of the Arc-Anode Attachment Area by Utilizing a High-Speed Camera, *PPT*, 2019, **3**(1), p 1-4
30. J. Schein, J. Zierhut, M. Dzulko, G. Forster, and K.D. Landes, Improved Plasma Spray Torch Stability Through Multi-electrode Design, *Contrib. Plasma Phys.*, 2007, **47**(7), p 498-504
31. L.-J. Marqués, G. Forster, and J. Schein, Multi-Electrode Plasma Torches: Motivation for Development and Current State-of-the-Art, *TOPPJ*, 2009, **2**(1), p 89-98

32. N. Otsu, A Threshold Selection Method from Gray-Level Histograms, *IEEE Trans. Syst. Man Cybern.*, 1979, **9**(1), p 62-66
33. E.R.G. Eckert, E. Pfender, and S.A. Wutzke, Study of Electric Arc Behavior with Superimposed Flow, *AIAA Journal*, 1967, **5**(4), p 707-713
34. V. Rat, F. Mavier, and J.-F. Coudert, Electric Arc Fluctuations in DC Plasma Spray Torch, *Plasma Chem. Plasma Process.*, 2017, **37**(3), p 549-580
35. C. Caruyer, S. Vincent, E. Meillot, J.-P. Caltagirone, and D. Damiani, Analysis of the Unsteadiness of a Plasma Jet and the Related Turbulence, *Surf. Coat. Technol.*, 2010, **205**(4), p 1165-1170
36. K. Bobzin, M. Öte, J. Schein, S. Zimmermann, K. Möhwald, and C. Lummer, Modelling the Plasma Jet in Multi-arc Plasma Spraying, *J. Therm. Spray Technol.*, 2016, **25**(6), p 1111-1126
37. K. Bobzin, M. Öte, J. Schein, and S. Zimmermann, Numerical Study on Plasma Jet and Particle Behavior in Multi-arc Plasma Spraying, *J. Therm. Spray Technol.*, 2017, **26**(5), p 811-830
38. J.R. Fincke and W.D. Swank, Measurement of Particle Size, Velocity and Temperature in the Plasma Spray Coating Process, Gas-Solid Flows 1991, in *Presented at the First ASME JSME Fluids Engineering Conference Portland, Oregon, June 23-27*, ed. D.E. Stock. American Society of Mechanical Engineers, 1991, p 97-102
39. P.L. Fauchais, M. Vardelle, A. Vardelle, L. Bianchi, and A.C. Léger, Parameters Controlling the Generation and Properties of Plasma Sprayed Zirconia Coatings, *Plasma Chem. Plasma Process.*, 1996, **16**(1), p 99-125
40. M. Vardelle, A. Vardelle, P.L. Fauchais, K.-I. Li, B. Dussoubs, and N.J. Themelis, Controlling Particle Injection in Plasma Spraying, *J. Therm. Spray Technol.*, 2001, **10**(2), p 267-284

**Publisher's Note** Springer Nature remains neutral with regard to jurisdictional claims in published maps and institutional affiliations.